Chapter 7

Interior first order resonance of Sun-Saturn system in ERTBP

7.1 Introduction

In this chapter, the first order interior resonant orbits in the photogravitational Sun-Saturn ERTBP are computed using the method of PSS. Interior resonance is a particular type of orbit-orbit resonance in which the spacecraft spends the majority of the time inside the orbit of the second primary with its semi-major axis smaller than the semi-major axis of the second primary. There are several examples of first order interior resonance in solar system. The 2:1 Io-Europa resonance of Galilean satellites of Jupiter is an example of first order interior resonance. Also, Neptune and Pluto are in 3:2 orbit-orbit resonance, satellites Enceladus and Dione are in 3:2 mean motion resonance, and Titan and Hyperion are in 4:3 orbit-orbit resonance. The 2:1 resonant perturbations of Mimas creates a gap between the rings A and B of Saturn. The formation of rings of Saturn and the gaps in the radial distribution of the asteroid orbits can be explained using the phenomenon of resonance (Murray and Dermott (1999)).

In CRTBP framework, Safiya Beevi and Sharma (2012a) have computed first order interior and exterior resonant orbits in the Saturn-Titan system and studied the effects of oblateness of the Saturn on resonant orbits. Many researchers have obtained first and higher order resonant orbits in different CRTBP systems using PSS method (Merritt and Valluri (1999), Klokočník et al. (2013), Yu and Baoyin (2013), Antoniadou and Voyatzis (2014), Pathak et al. (2016), Pushparaj and Sharma (2017), and Pathak et al. (2019a)). Recently, Patel et al. (2021) have obtained three different families of first order resonant orbits in the framework of Saturn-Titan CRTBP and Patel et al. (2022b) have analyzed the stability of these orbits.

In this chapter, autonomous system of equations (1.49) representing the motion of infinitesimal body in ERTBP framework is used to generate the PSS using which the resonant periodic orbits are computed. The variations in parameters of resonant orbits due to non-zero eccentricity of the orbit of the primaries, solar radiation pressure and Jacobi constant are studied.

7.2 Resonance Ratio

In interior resonance, the ratio of mean motions, $p : s$, is such that $p > s$. The notation $p + s : p$ shall be used to denote the resonance ratio. As described in Section 6.2, using PSS and two-body approximations, the ratio $p + s : p$ can be determined. PSS for different values of e, q and C are generated by solving equations (1.49) using RKG method by considering $x \in [0, 1]$ with a fixed step size of 0.001. The solutions satisfying $y = 0$ and $y' > 0$ are plotted on the xx' plane which forms the PSS. From PSS, the centres of islands are identified which are locations (x) of resonant orbits. The velocity (v), angular momentum (h), eccentricity (e_s) and semi-major axis (a_s) of spacecraft moving in resonant orbits are calculated with the aid of equations (6.1) and (6.2). The resonance ratio $p + s : p$ can be obtained using

$$\frac{p+s}{p} = \left(\frac{a}{a_s}\right)^{3/2}, \tag{7.1}$$

where a is the semi-major axis of the orbit of the primaries. In interior resonance also the number s provides the order of resonance. Further, the configuration is repeated after every $p+s$ orbits of the spacecraft. In interior resonance, the orbits of spacecraft have $p + s$ external loops.

7.3 Results and Discussion

For studying the effects of eccentricity of primaries' orbit, solar radiation pressure and Jacobi constant on parameters of interior resonant orbits, the Sun-Saturn system with the Sun as a source of radiation is considered. In Fig. 7.1, PSS in Sun-Saturn system for $e = 0.052, q = 0.98$ and $C = 2.88$ is given. Here, $e = 0.052$ is the eccentricity of the orbit of the Saturn round the Sun. For selecting initial conditions for numerical integration, constant values of q and C are considered in equation (1.51) for different values of e. The PSS in Fig. 7.1 has four islands containing the first order interior resonant orbits.

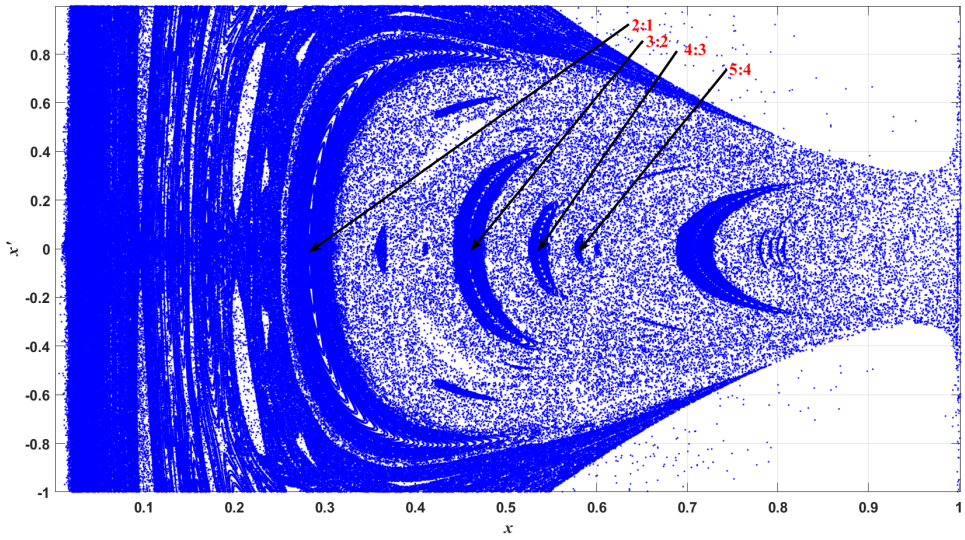

FIGURE 7.1: PSS of Sun-Saturn system for $e = 0.052, q = 0.98$ and $C = 2.88$

Periodic orbits with 2:1, 3:2, 4:3 and 5:4 interior resonances (located from PSS in Fig. 7.1) are shown in Fig. 7.2. Location (x) of periodic orbit is identified as a centre of the island from the figures plotted for PSS. In the study of first order interior resonance, orbits having 2, 3, 4 and 5 external loops are obtained.

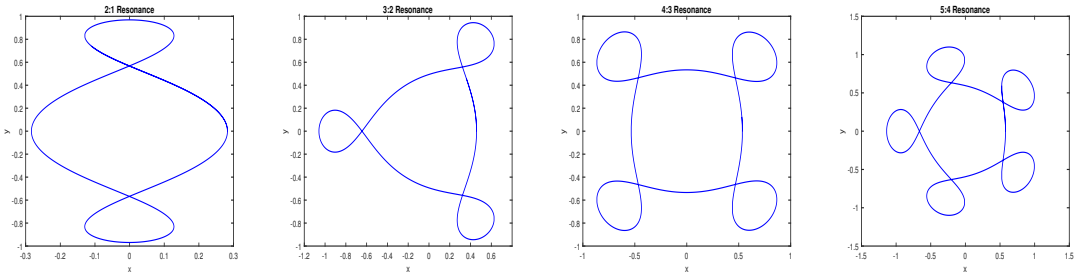

FIGURE 7.2: First order interior resonant orbits corresponding to Fig. 7.1

In Tables 7.1-7.3, location (x), period (T), semi-major axis (a_s), eccentricity (e_s), ratio $(a/a_s)^{3/2}$ and corresponding value of $p + s : p$ of resonant orbits for different values of e, q and C are given. From these tables, it can be observed that orbits having 2, 3, 4 and 5 external loops are obtained for different values of e and q.

7.3.1 Effects of eccentricity of primaries' orbit

All orbital parameters of resonant orbits get altered due to non-zero eccentricity of the orbit of the primaries. For analyzing variations in locations (x), periods (T), semi-major axis (a_s) and eccentricity(e_s) of resonant orbits, four different values of e in the

range $[0.00, 0.09]$ are considered. Here, $e = 0$ corresponds to CRTBP.

The changes in locations of $3 : 2$ resonant orbits due to increase in the value of e for three different values of q are shown in Fig. 7.3. Here, $C = 2.90$ is considered. With the increase in e, these orbits shift towards the Sun. From Tables 7.1-7.3, it can be observed that all orbits shift towards the Sun with the increase in the value of e. Further, first order interior resonant orbits lie on the left side of the f-famillt orbits.

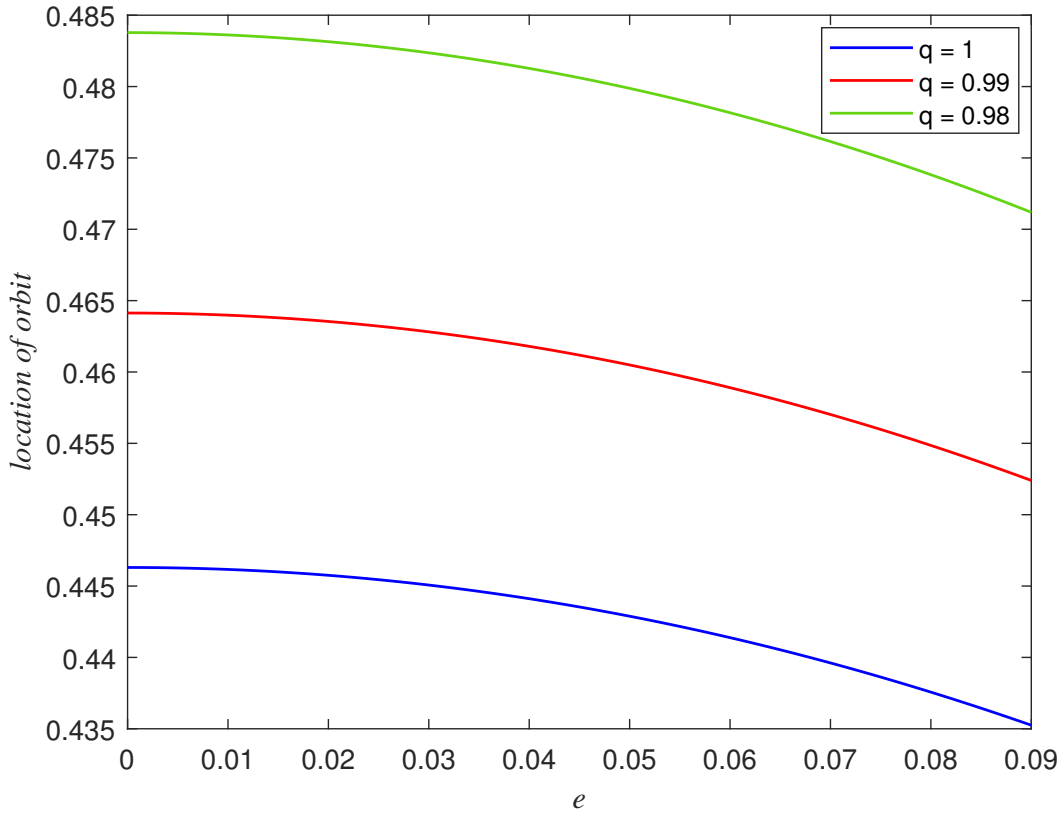

FIGURE 7.3: Variation in location of $3 : 2$ resonant orbits for $C = 2.90$

The variation in period of spacecraft's orbit can be analyzed from Tables 7.1-7.3. With the increase in the value of e, period of 2:1, 3:2, 4:3 and 5:4 resonant orbits increase. In Fig. 7.4(A), the variation in semi-major axis of $5 : 4$ resonant orbits for $C = 2.92$ is shown graphically. It can be observed that a_s is a monotonically increasing function of e. Further, this functional relation is non-linear. From the data of Tables 7.1-7.3, it can be concluded that the semi-major axis of $2 : 1, 3 : 2$ and $4 : 3$ resonant orbits also increase with the increase in the value of e. Fig. 7.4(B) shows that as the value of e increases, the eccentricity (e_s) of $5 : 4$ resonant orbits also increase. Here, $C = 2.92$ is considered. It can be observed from Tables 7.1-7.3 that e_s increases with the increase in e for all first order interior resonant orbits.

TABLE 7.1: Orbital Parameters of resonant orbit for $C = 2.89$ and $q = 1$

No. of Loops	e	x	T	a_s	e_s	$(a/a_s)^{3/2}$	$p+s:p$
2	0.000	0.26951	6.2828	0.6299	0.5717	2.0236	2:1
	0.030	0.26882	6.2845	0.6308	0.5734	2.0189	
	0.052	0.26746	6.2878	0.6328	0.5769	2.0094	
	0.090	0.26337	6.2974	0.6390	0.5874	1.9803	
3	0.000	0.43692	12.5663	0.7634	0.4273	1.5166	3:2
	0.030	0.43570	12.5708	0.7640	0.4294	1.5147	
	0.052	0.43331	12.5807	0.7654	0.4335	1.5107	
	0.090	0.42617	12.6083	0.7695	0.4458	1.4986	
4	0.000	0.51035	18.8538	0.8269	0.3825	1.3452	4:3
	0.030	0.50887	18.8623	0.8275	0.3847	1.3439	
	0.052	0.50593	18.8794	0.8285	0.3890	1.3413	
	0.090	0.49719	18.9272	0.8319	0.4020	1.3331	
5	0.000	0.55318	25.1593	0.8670	0.3616	1.2530	5:4
	0.030	0.55157	25.1695	0.8675	0.3639	1.2519	
	0.052	0.54850	25.1951	0.8686	0.3682	1.2495	
	0.090	0.53952	25.2679	0.8723	0.3811	1.2417	

TABLE 7.2: Orbital Parameters of resonant orbit for $C = 2.89$ and $q = 0.99$

No. of Loops	e	x	T	a_s	e_s	$(a/a_s)^{3/2}$	$p+s:p$
2	0.000	0.27988	6.2827	0.6277	0.5537	2.0338	2:1
	0.030	0.27919	6.2845	0.6287	0.5555	2.0293	
	0.052	0.27777	6.2878	0.6306	0.5590	2.0202	
	0.090	0.27354	6.2973	0.6364	0.5697	1.9924	
3	0.000	0.45398	12.5654	0.7608	0.4029	1.5242	3:2
	0.030	0.45271	12.5706	0.7615	0.4051	1.5223	
	0.052	0.45017	12.5805	0.7627	0.4094	1.5186	
	0.090	0.44261	12.6080	0.7666	0.4223	1.5071	
4	0.000	0.53070	18.8521	0.8241	0.3557	1.3521	4:3
	0.030	0.52912	18.8610	0.8246	0.3580	1.3509	
	0.052	0.52596	18.8778	0.8256	0.3626	1.3484	
	0.090	0.51660	18.9259	0.8288	0.3763	1.3408	
5	0.000	0.57460	25.1508	0.8632	0.3340	1.2613	5:4
	0.030	0.57286	25.1623	0.8637	0.3364	1.2603	
	0.052	0.56950	25.1896	0.8647	0.3411	1.2580	
	0.090	0.55946	25.2603	0.8677	0.3549	1.2514	

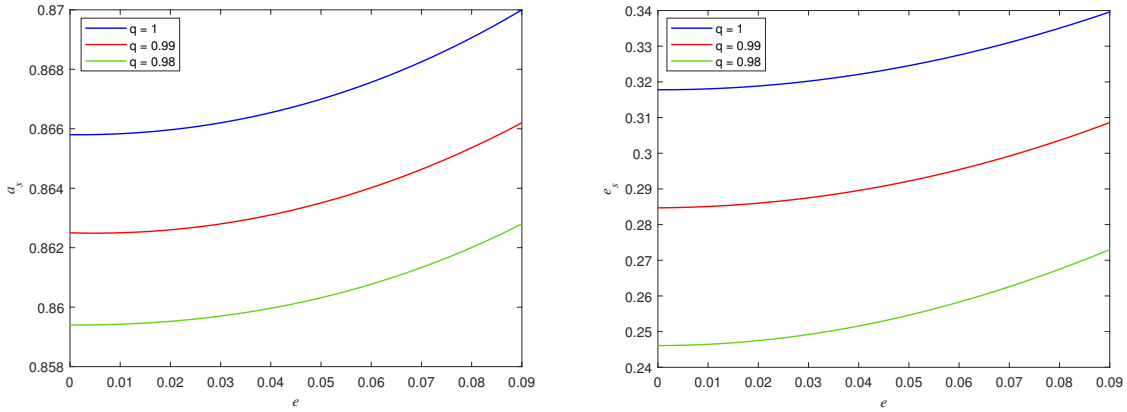

(A) Variation in a_s (B) Variation in e_s

FIGURE 7.4: Variation in a_s and e_s against variation in e for $5:4$ resonant orbits for $C = 2.92$

TABLE 7.3: Orbital Parameters of resonant orbit for $C = 2.89$ and $q = 0.98$

No. of Loops	e	x	T	a_s	e_s	$(a/a_s)^{3/2}$	$p+s:p$
2	0.000	0.29095	6.2826	0.6256	0.5345	2.0441	2:1
	0.030	0.29022	6.2844	0.6265	0.5363	2.0398	
	0.052	0.28875	6.2878	0.6283	0.5400	2.0312	
	0.090	0.28435	6.2972	0.6338	0.5509	2.0045	
3	0.000	0.47270	12.5645	0.7583	0.3762	1.5319	3:2
	0.030	0.47136	12.5702	0.7589	0.3785	1.5301	
	0.052	0.46864	12.5800	0.7601	0.3830	1.5266	
	0.090	0.46059	12.6079	0.7637	0.3965	1.5156	
4	0.000	0.55345	18.8508	0.8213	0.3258	1.3590	4:3
	0.030	0.55170	18.8586	0.8218	0.3283	1.3579	
	0.052	0.54825	18.8753	0.8227	0.3332	1.3556	
	0.090	0.53817	18.9258	0.8257	0.3478	1.3483	
5	0.000	0.59916	25.1452	0.8598	0.3028	1.2688	5:4
	0.030	0.59724	25.1573	0.8602	0.3054	1.2679	
	0.052	0.59339	25.1804	0.8610	0.3105	1.2661	
	0.090	0.58232	25.2542	0.8638	0.3255	1.2600	

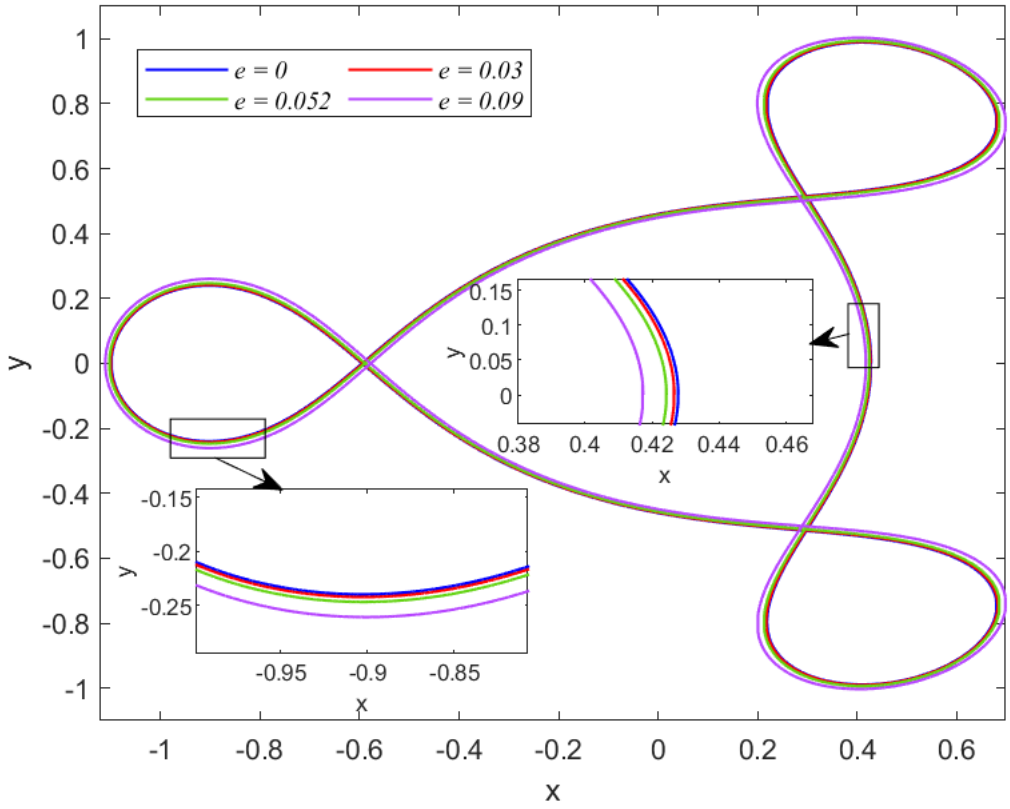

FIGURE 7.5: Variation in size and shape of $3:2$ resonant orbits with $q = 1$ and $C = 2.88$

The variation in the size of $3:2$ resonant orbits for four different values of e is shown in Fig. 7.5. The orbits in blue, red, green and lavender colours correspond to $e = 0, 0.03, 0.052$ and 0.09, respectively. In Fig. 7.5, $q = 1$ and $C = 2.88$ is considered for plotting the orbits. It can be observed that due to increase in the value of e, these orbits shrink while the loops of these orbits expand. Similar effect of eccentricity of the orbit of the primaries is observed on first order resonant orbits having 2, 4 and 5 external loops.

7.3.2 Effects of radiation pressure

For studying the effects of solar radiation pressure on various parameters of resonant orbits, three different values of q in the interval [0.98, 1.00] are considered. The value $q = 1$ means that the perturbation due to solar radiation pressure is neglected. In Fig. 7.3, the change in the locations of $3:2$ resonant orbits corresponding to $q = 1.00, 0.99$ and 0.98 is shown with blue, red and green curves, respectively. It can be observed that as the solar radiation pressure increases, periodic orbits move towards the Saturn. Similar result holds true for $2:1, 4:3$ and $5:4$ resonant orbits (Tables 7.1-7.3).

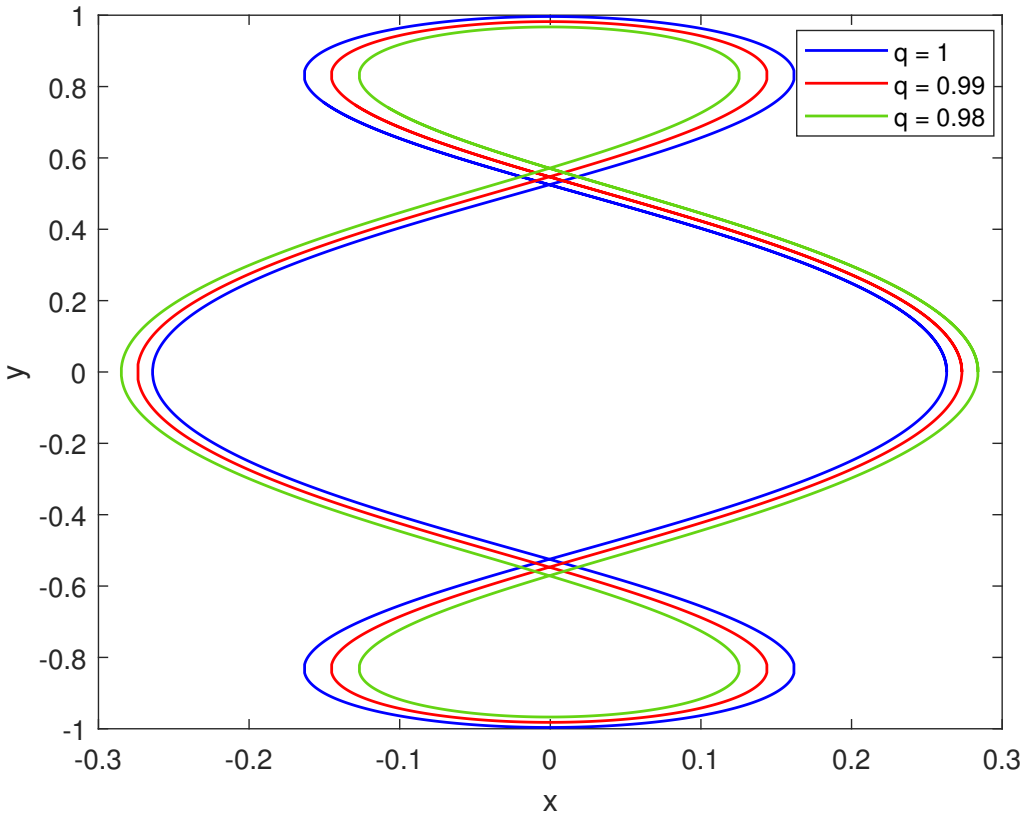

FIGURE 7.6: Variation in size and shape of $2:1$ resonant orbits with $e = 0.03$ and $C = 2.88$

From Tables 7.1-7.3, it is clear that period, semi-major axis and eccentricity of orbits decrease due to increase in solar radiation pressure. Variations in a_s and e_s for $5:4$ resonant orbits for $C = 2.92$ are shown in Fig. 7.4 with blue, red and green curves corresponding to $q = 1.00, 0.99$ and 0.98, respectively. The semi-major axis and eccentricity of orbits decrease with the increase in the solar radiation pressure. Also, from Tables 7.1-7.3, it can be concluded that for first order exterior resonant orbits, a_s and e_s are decreasing functions of solar radiation pressure for all values of e and C. Pathak et al. (2019b) have obtained first order interior resonant periodic orbits for the Sun-Earth and Sun-Mars photogravitational CRTBP with oblateness. They have obtained similar effects of solar radiation pressure on parameters of resonant orbits which shows the effect of solar radiation pressure is similar in CRTBP and ERTBP framework.

Variation in size and shape of orbits due to variation in solar radiation pressure is shown in Fig. 7.6 for $e = 0.03$ and $C = 2.88$. Orbits in blue, red and green correspond

to $q = 1.00, 0.99$ and 0.98, respectively. It can be observed that orbits enlarge and loops of these orbits shrink due to increase in solar radiation pressure.The effects of solar radiation pressure on parameters of resonant orbits are similar in different Sun-Planet systems (Pathak et al. (2019b)).

7.3.3 Effects of Jacobi constant

The effects of Jacobi constant on parameters of resonant orbits are studied by considering five different values of C in the interval [2.88, 2.92]. In Table 7.4, the data of locations, periods, semi major axis (a_s) and eccentricity (e_s) of resonant orbits for different values of C corresponding to $e = 0.052$ and $q = 0.99$ are given. It can be observed from Table 7.4 that as the value of Jacobi constant increases, all resonant periodic orbits shift towards the Saturn. Further, the semi-major axis, a_s, and eccentricity, e_s, of spacecraft's orbit are decreasing functions of C.

The period of orbits is not a monotonic function of C for $2 : 1$ and $3 : 2$ resonant orbits while for $4 : 3$ and $5 : 4$ resonant orbits, it is a monotonically decreasing function of Jacobi constant (Table 7.4). These results agree with the results of Pathak et al. (2019b). The variation in the size and shape of orbits corresponding to five different values of C are shown in Fig. 7.7. Here, $4 : 3$ resonant orbits are plotted by taking $e = 0.09$ and $q = 0.99$ for analyzing the variation in size and shape of orbits. In Fig. 7.7, orbits in blue, red, green, lavender and black colours correspond to $C = 2.88, 2.89, 2.90 2.91$ and 2.92, respectively. It is clear from Fig. 7.7 that orbits enlarge while the loops of orbits shrink due to increase in the value of Jacobi constant.

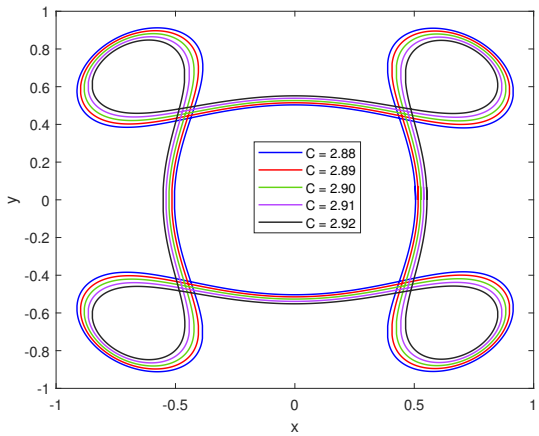

FIGURE 7.7: Variation in size and shape of $4 : 3$ resonant orbits with $e = 0.09$ and $q = 0.99$

TABLE 7.4: Orbital Parameters of resonant orbits for $e = 0.052$ and $q = 0.99$

No. of Loops	C	x	T	a_s	e_s
2	2.88	0.27189	6.2877	0.63062	0.5684
	2.89	0.27777	6.2878	0.63055	0.5590
	2.90	0.28379	6.2878	0.63048	0.5494
	2.91	0.28996	6.2877	0.63041	0.5396
	2.92	0.29630	6.2877	0.63035	0.5295
3	2.88	0.44052	12.5805	0.76276	0.4221
	2.89	0.45017	12.5805	0.76271	0.4094
	2.90	0.46019	12.5802	0.76267	0.3962
	2.91	0.47061	12.5797	0.76261	0.3825
	2.92	0.48152	12.5798	0.76259	0.3682
4	2.88	0.51448	18.8786	0.82569	0.3766
	2.89	0.52595	18.8778	0.82561	0.3626
	2.90	0.53797	18.8771	0.82554	0.3480
	2.91	0.55061	18.8761	0.82548	0.3326
	2.92	0.56391	18.8741	0.82541	0.3165
5	2.88	0.55735	25.1916	0.86516	0.3555
	2.89	0.56950	25.1896	0.86469	0.3411
	2.90	0.58230	25.1847	0.86425	0.3259
	2.91	0.59595	25.1825	0.86394	0.3099
	2.92	0.61044	25.1762	0.86364	0.2928

7.4 Conclusions

In this chapter, the first order interior resonant orbits are computed in the photogravitaional Sun-Saturn ERTBP using the technique of PSS. The analysis of PSS shows that these orbits lie on the left-side of f-family orbits. The effects of eccentricity of orbit of primaries, radiation pressure and Jacobi constant on parameters of resonant orbits are studied. It is observed that four types of interior first order resonant orbits having 2, 3, 4 and 5 external loops exist for values of Jacobi constant varying in the range $[2.88, 2.92]$.

It is observed that due to increase in the value of eccentricity of the orbit of the primaries, all first order resonant orbits shift towards the Sun and their period, eccentricity and semi-major axis increase. Due to perturbation of radiation pressure, orbits shift towards the Saturn and expand in size. Period, eccentricity and semi-major axis of these orbits decrease due to radiation of the Sun. With the increase in Jacobi constant, first order resonant orbits move closer to the Saturn and enlarge.

The eccentricity and semi major axis of these orbits decrease due to increase in the value of Jacobi constant. Also, it is observed that period of interior resonant orbits is a non-monotonic function of Jacobi constant for 2 and 3 loops orbits while it is a monotonically decreasing function of Jacobi constant for 4 and 5 loops orbits.